

Cas A and the Crab Were Not Stellar Binaries At Death

C. S. Kochanek^{1,2},

¹ *Department of Astronomy, The Ohio State University, 140 West 18th Avenue, Columbus OH 43210*

² *Center for Cosmology and AstroParticle Physics, The Ohio State University, 191 W. Woodruff Avenue, Columbus OH 43210*

12 November 2018

ABSTRACT

The majority of massive stars are in binaries, which implies that many core collapse supernovae (ccSNe) should be binaries at the time of the explosion. Here we show that the three most recent, local (visual) SNe (the Crab, Cas A and SN 1987A) were not binaries, with limits on the initial mass ratios of $q = M_2/M_1 \lesssim 0.1$. No quantitative limits have previously been set for Cas A and the Crab, while for SN 1987A we merely updated existing limits in view of new estimates of the dust content. The lack of stellar companions to these three ccSNe implies a 90% confidence upper limit on the $q \gtrsim 0.1$ binary fraction at death of $f_b < 44\%$. In a passively evolving binary model (meaning no binary interactions), with a flat mass ratio distribution and a Salpeter IMF, the resulting 90% confidence upper limit on the initial binary fraction of $F < 63\%$ is in considerable tension with observed massive binary statistics. Allowing a significant fraction $f_M \simeq 25\%$ of stellar binaries to merge reduces the tension, with $F < 63(1 - f_M)^{-1\%} \simeq 81\%$, but allowing for the significant fraction in higher order systems (triples, etc.) reintroduces the tension. That Cas A was not a stellar binary at death also shows that a massive binary companion is not necessary for producing a Type IIb SNe. Much larger surveys for binary companions to Galactic SNe will become feasible with the release of the full Gaia proper motion and parallax catalogs, providing a powerful probe of the statistics of such binaries and their role in massive star evolution, neutron star velocity distributions and runaway stars.

Key words: stars: massive – supernovae: general – supernovae: individual: Cas A, Crab, SN 1987A

1 INTRODUCTION

A large fraction of massive stars appear to be in binaries (see the reviews by Duchêne & Kraus 2013 and Moe & Di Stefano 2016). Kobulnicky et al. (2014) estimate that 55% are in binaries with $P < 5000$ days and mass ratios of $0.2 < q < 1$, while Sana et al. (2012) estimate that 69% are in binaries and that two-thirds of these will undergo some form of interaction. Moe & Di Stefano (2016) find that only $16 \pm 8\%$ of the $9\text{--}16M_\odot$ stars that will dominate the SN rate are single, and that they have an average multiplicity (companions per primary) of 1.6 ± 0.2 .

Mass transfer, mass loss and mergers then significantly modify the subsequent evolution of the system (e.g., Eldridge et al. 2008, Sana et al. 2012). This will, in turn, modify the properties of any resulting supernovae (SNe) over the expectations for isolated stars. For example, the numbers of stripped Type Ibc SNe and the limits on their progenitor stars both suggest that many are stripped through binary mass transfer rather than simply wind (or other) mass loss (e.g., De Donder & Vanbeveren 1998, Eldridge et al.

2008, Smith et al. 2011, Eldridge et al. 2013). There are many theoretical studies exploring the stripped Type IIb, Ib and Ic SNe in the context of binary evolution models (e.g., Yoon et al. 2010, Yoon et al. 2012, Claeys et al. 2011, Dessart et al. 2012, Benvenuto et al. 2013, Kim et al. 2015, Yoon et al. 2017), as well as models for the effects of binary evolution on electron capture SNe (e.g., Moriya & Eldridge 2016).

Discussions of the binary companions to local core collapse SNe have largely focused on understanding runaway B stars (e.g., Blaauw 1961, Gies & Bolton 1986, Hoogerwerf et al. 2001, Tetzlaff et al. 2011) and the contribution of binary disruption to the velocities of neutron stars (NS) (e.g., Gunn & Ostriker 1970, Iben & Tutukov 1996, Cordes & Chernoff 1998, Faucher-Giguère & Kaspi 2006). van den Bergh (1980) seems to have been the first to search supernova remnants (SNRs) for runaway stars by looking for a statistical excess of O stars close to the centers of 17 SNRs and finding none. Guseinov et al. (2005) examined 48 SNRs for O or B stars using simple color, magnitude and proper motion selection cuts to produce a list of candidates

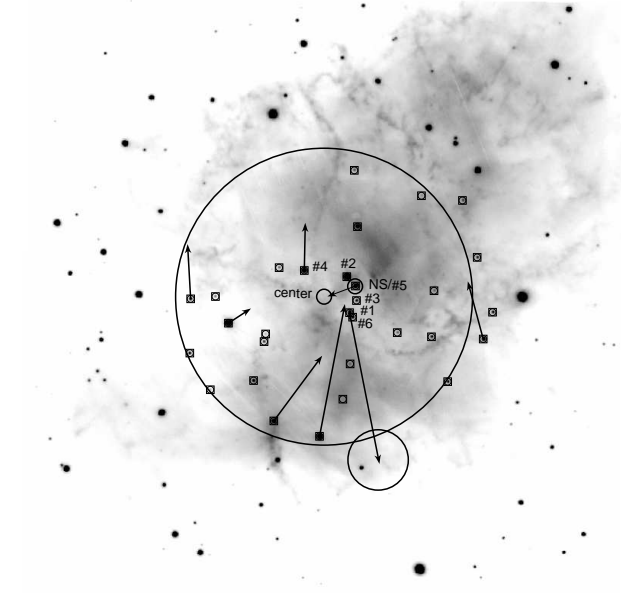


Figure 1. Coadded grizy PS1 image of the Crab. The position of the geometric center of the remnant (“center”) and the neutron star are indicated by 3’’ radius green circles. The larger green circle shows the region within 60’’ of the center. The 30 stars within 60’’ of either the center or the NS are marked, and the six closest to the center are numbered in order of their distance from the center. The NS is star #5. The arrows show the predicted positions of sources with proper motions at the time of the SN. As expected, the predicted position of the pulsar is close to the center of the SNR. Seven stars have proper motions in NOMAD with uncertainties in their back-projected positions of approximately 12’’ as shown by the circle at the head of one of the proper motion vectors. At a distance of 2.0 kpc, a star will have moved $10''.1(v/100 \text{ km/s})$ since the SN, so the 60’’ search radius corresponds to a velocity of roughly 600 km/s.

based on the USNO A2 catalog (Monet et al. 1998). None of these systems have been investigated in any quantitative detail. Dincel et al. (2015) identify a good candidate in the $\sim 3 \times 10^4$ year old SNR S147 containing PSR J0538+2817 and argue that it was also likely to have been an interacting binary. Considerably more effort has been devoted to searching for single degenerate companions to Type Ia SN (e.g., Schweizer & Middleditch 1980 Ruiz-Lapuente et al. 2004, Ihara et al. 2007, González Hernández et al. 2012, Schaefer & Pagnotta 2012).

Searches for binary companions to core-collapse SNe in external galaxies are more challenging because the companion is generally significantly fainter than the progenitor (see Kochanek 2009). The Type IIb SN 1993J is probably the best case (Maund et al. 2004, Fox et al. 2014), while the existence of a companion to the Type IIb SN 2011dh is debated, with Folatelli et al. (2014) arguing for a detection and Maund et al. (2015) arguing that the flux may be dominated by late time emission from the SN. There is some evidence of a blue companion for the Type IIb SNe 2001ig (Ryder et al. 2006) and SN 2008ax (Crockett et al. (2008)). There are limits on the existence companions to the Type Ic SNe 1994I (Van Dyk et al. 2016) and SN 2002ap (Crockett et al. 2007) and the Type IIP SNe 1987A (Graves et al. 2005), SN 2005cs (Maund et al.

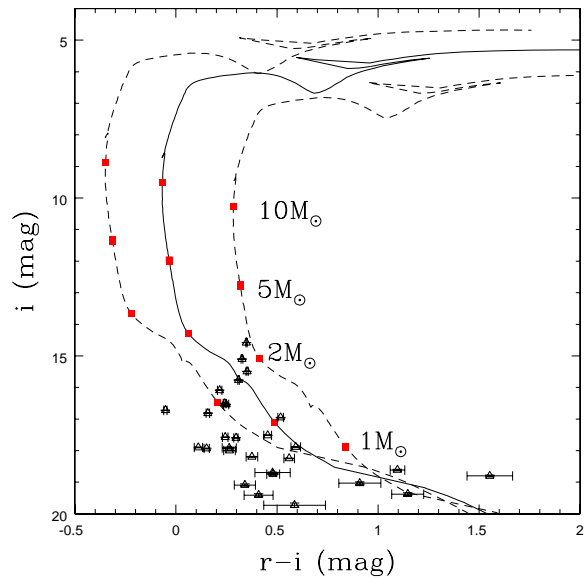


Figure 2. The $r/r-i$ CMD of the stars within 60’’ of the center of the Crab SNR or NS. The solid curve shows the PARSEC (Bressan et al. 2012) isochrone for Solar metallicity stars with an age of $10^{7.3}$ years at a distance of 2 kpc and with an extinction of $E(B-V) = 0.4$ mag. The dashed curves show the effect of reducing (raising) the extinction to $E(B-V) = 0$ mag (0.9 mag). Uncertainties in the distance modulus are much less important, corresponding to vertical shifts of ± 0.5 mag. Red filled squares on the isochrones mark stars with masses of 1, 2, 5 and $10 M_{\odot}$.

2005, Li et al. 2006), and SN 2008bk (Mattila et al. 2008). All of these limits assume that the SNe made little dust, an issue we discuss further in Kochanek (2017) and consider in more detail for SN 1987A below.

Kochanek (2009) examined the statistical properties expected for surviving binary companions to SNe assuming passively evolving systems (i.e. no binary interactions). As already noted, the companions are generally significantly fainter than the exploding star, although this is frequently not the case for stripped SN progenitors – for Type Ibc SNe, it should not be surprising to find that the binary companion is more visually luminous than the SN progenitor. This point is of considerable importance for the one candidate Type Ib progenitor iPTF13bvn (Cao et al. 2013, Groh et al. 2013, Bersten et al. 2014, Fremling et al. 2014, Eldridge et al. 2015, Eldridge & Maund 2016, Folatelli et al. 2016). If the initial binary fraction is F , then the fraction of passively evolving binaries that are in stellar binaries at death is

$$f_b = \frac{F}{1 + F f_q} \quad \text{where} \quad f_q = \int_{q_{min}}^{q_{max}} q^{x-1} P(q) dq, \quad (1)$$

$x \simeq 2.35$ is the slope of the initial mass function (IMF), $q_{min} \leq q = M_2/M_1 \leq q_{max} \leq 1$ is the mass ratio and $P(q)$ with $\int dq P(q) \equiv 1$ is the distribution of mass ratios. For a Salpeter IMF and a flat $P(q)$ distribution extending over $0 \leq q \leq 1$, $f_q = 0.426$ and the fraction of SNe in stellar binaries at death is 23%, 41%, 57% and 70% for initial binary fractions of $F = 25\%$, 50%, 75% and 100%, respectively. Essentially, only the explosions of primaries occur in stellar binaries, so the fraction of SNe in stellar binaries is less than

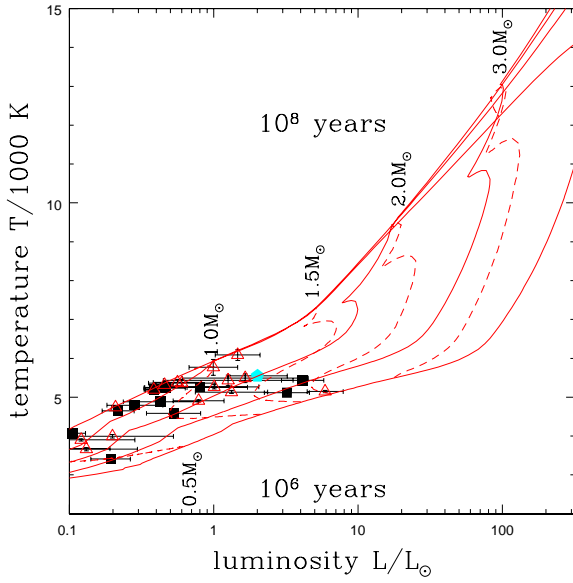


Figure 3. The luminosities and temperatures of the stars if at the distance of the Crab and constrained by the extinction prior. Filled black squares mark the stars that could be at the distance of the Crab ($\chi^2_2 < \chi^2_0 + 4$) and an association is not ruled out by the available proper motions. Open red triangles are for stars that either cannot lie at the distance of the Crab ($\chi^2_2 > \chi^2_0 + 4$) or have a proper motion inconsistent with an association. The pulsar, fit as a star, is indicated by the filled, cyan pentagon. The solid lines show isochrones with ages of 10^6 , $10^{6.5}$, 10^7 , $10^{7.5}$ and 10^8 years while the dashed lines show the tracks for 0.5, 1.0, 1.5, 2.0 and $3.0M_\odot$ stars over this range of times.

the initial fraction of binaries because some of the SNe are the explosions of secondaries. Binary evolution, particularly stellar mergers, then adds further complications, as does the prevalence of triples and other higher order systems.

For a supernova of a given age, we need an estimate of the radius inside the SNR that needs to be searched. Guseinov et al. (2005) simply used a fixed 1/6 of the diameter of the remnant as cataloged by Green (2014) (for the most recent version). Observed runaway stars have typical velocities of 50 km/s or less (e.g., Tetzlaff et al. 2011) and theoretical studies find that it is difficult for binaries to produce velocities of more than a few 100 km/s (e.g., Cordes & Chernoff 1998, Eldridge et al. 2011). This has a simple explanation in terms of stellar structure because the maximum (circular) orbital velocity of a secondary star is limited by

$$v_2^2 < \frac{GM_1}{1+q} \left[\frac{4\pi\sigma T_1^4}{L_1} \right]^{1/2} \left[1 + \left(\frac{L_2}{L_1} \right)^{1/2} \frac{T_1^2}{T_2^2} \right]^{-1} \quad (2)$$

where the mass ratio $q = M_2/M_1$ could be > 1 here, the semi-major axis is set to the sum of the two stellar radii, and we have expressed the radii in terms of the stellar luminosities and effective temperatures. The highest possible companion velocity is achieved for a low mass ($q \rightarrow 0$) and low luminosity $L_2/L_1 \rightarrow 0$ companion. This allows the simple upper limit on the companion's velocity of

$$v < 50M_{10}^{1/2} T_{3.5} L_{4.7}^{-1/4} \text{ km/s} \quad (3)$$

where the scalings of $M_1 = 10M_{10}M_\odot$, $T_1 = 10^{3.5}T_{3.5}$ K and

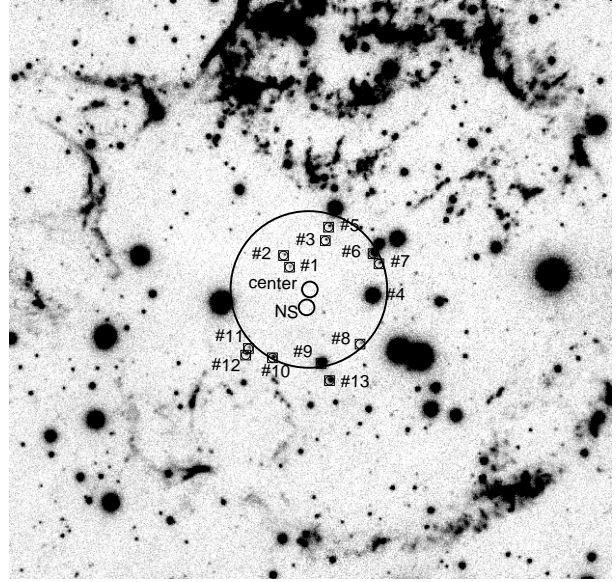


Figure 4. Coadded grizy PS1 image of Cas A. The position of the geometric center of the remnant (“center”) and the neutron star are indicated by $3''.0$ radius circles. The larger circle shows the region within $30''.0$ of the center. The 13 PS1 stars lying within $30''.0$ of either the geometric center or the neutron star are marked and labeled in order of their distance from the center. None of the stars have proper motion measurements in NOMAD. Stars #4, #9 and #13 have proper motions in HSOY but the shift in position to the time of the SN is too small to display. At a distance of 3.4 kpc, a star will have moved $2''.1(v/100 \text{ km/s})$ since the SN, so the $30''.0$ search radius corresponds to a velocity of roughly 1500 km/s

$L_1 = 10^{4.7}L_{4.7}L_\odot$ are chosen to match the end point of a $10^{7.4}$ year PARSEC (Bressan et al. 2012) stellar isochrone. The scaling with mass and luminosity is very weak¹, so the only important variable is the temperature of the primary. For the typical red supergiant progenitors of Type II SNe (see Smartt 2009), we expect very low velocities, $v < 50$ km/s. In the rare cases like SN 1987A where the primary is a blue supergiant at the time of explosion, the maximum companion velocity is still $v \lesssim 300$ km/s.

Companions to stripped, Type Ibc SNe can have higher velocities because of the very high progenitor temperatures. For these systems, the finite size of the secondary is important because the radius of the primary is $\sim R_\odot$, and the companion velocities can in theory reach $\sim 10^3$ km/s. This is only true if the system was an interacting binary because the orbit of the secondary must also shrink to be far smaller than even the initial size the primary. Such tightly bound binaries are less likely to be disrupted because the primary mass has to have been greatly reduced by mass loss and the orbital binding energy is larger than typical NS kick velocities (e.g., Cordes & Chernoff 1998). Theoretically, Eldridge et al. (2011), using binary population synthesis models that included such evolutionary paths, found that velocities above 300 km/s were very rare.

¹ For $L \propto M^x$, the velocity limit scales with primary mass as $v_1 \propto M^{1/2-x/4}$. For $x = 3$ ($x = 2$), this becomes $v_1 \propto M_1^{-1/4}$ ($v_1 \propto M_1^0$).

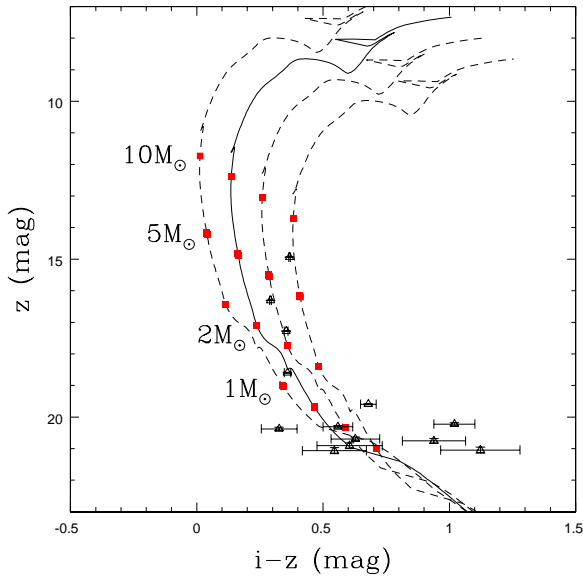


Figure 5. The $z/i-z$ CMD of the stars within $30''$ of the center of the Cas A SNR or the NS. The solid curve shows the PARSEC (Bressan et al. 2012) isochrone for Solar metallicity stars with an age of $10^{7.3}$ years at a distance of 3.4 kpc and with an extinction of $E(B-V) = 1.6$ mag ($A_V = 5.0$). The dashed curves show the effect of reducing the extinction to $A_V = 3.4$ or raising it to 6.5 or 8.0 mag. Uncertainties in the distance modulus are much less important, corresponding to vertical shifts of ± 0.2 mag. Red filled squares on the isochrones mark stars with masses of 1, 2, 5 and $10 M_\odot$.

Here we consider the three most recent visually observed, Local Group, core collapse SNe: the Crab, Cas A and SN 1987A. For Galactic SN, the Crab and Cas A have several advantages. Their youth means that the search areas are small, and the fact that they were visible by eye means that they have modest extinctions and, by extension, lie in regions with relatively low stellar densities for the Galaxy. We were unable to find any quantitative discussions of searches for binary companions to these two systems, but Guseinov et al. (2005) report no candidates in their qualitative survey of 48 SNRs. The Crab pulsar is observed in the optical/near-IR, but it is emission due to the pulsar and not from a surviving binary (e.g., Sandberg & Sollerman 2009, Scott et al. 2003). There have been a series of unsuccessful searches for an optical/near-IR counterpart to the NS in Cas A which rule out any bound system even at the level of a $M_2 \simeq 0.1 M_\odot$ dwarf companion (e.g., van den Bergh & Pritchett 1986, Kaplan et al. 2001, Ryan et al. 2001, Fesen et al. 2006). These studies also implicitly set strong limits on any unbound system, but the topic is never discussed in these papers. Graves et al. (2005) set very strong limits on the existence of a binary companion to SN 1987A but assumed there was very little dust obscuration created by the SN. More recent studies have shown that SN 1987A formed far more dust than assumed by Graves et al. (2005) and that it is concentrated towards the center of the remnant (Matsuura et al. 2011, Indebetouw et al. 2014, Matsuura et al. 2015), making it necessary to revisit these limits.

The Crab was almost certainly a Type II SNe due to the

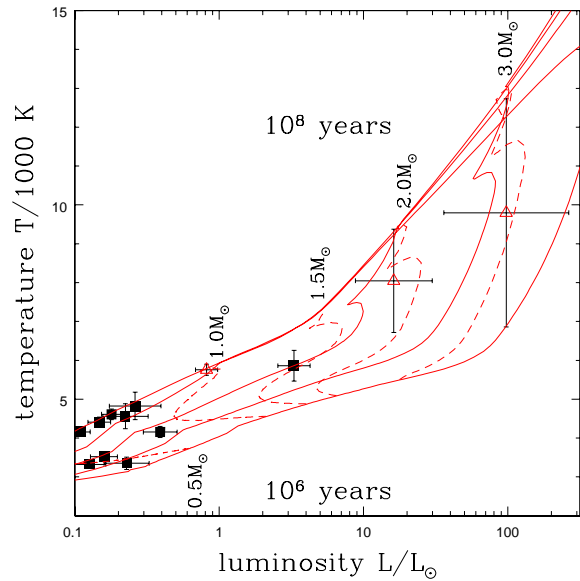


Figure 6. The luminosities and temperatures of the stars if at the distance of the Cas A and constrained by the extinction prior. Filled black squares mark the stars that could be at the distance of Cas A ($\chi^2_2 < \chi^2_0 + 4$) and not ruled out by proper motions. Open red triangles mark stars that cannot be at the distance of the Crab ($\chi^2_2 > \chi^2_0 + 4$) or an association is ruled out by the proper motions. In practice, the only star which is inconsistent with the distance (#13) is also ruled out by its proper motion. The solid lines show isochrones with ages of 10^6 , $10^{6.5}$, 10^7 , $10^{7.5}$ and 10^8 years while the dashed lines show the tracks for 0.5, 1.0, 1.5, 2.0 and $3.0 M_\odot$ stars over this range of times.

presence of significant amounts of hydrogen. However, the SNR appears to contain too little mass or energy for it to have been a normal Type II SN, suggesting it may have been an electron capture SN (see the review by Hester (2008) or the recent discussion by Smith (2013)). The binary models of Moriya & Eldridge (2016) would be one way of having such a low ejecta mass. Cas A is known to be a Type IIb thanks to spectra of light echoes from the SN (Krause et al. 2008, Rest et al. 2008, Rest et al. 2011, Finn et al. 2016). Single star evolution models generally have difficulty producing Type IIb SNe (e.g., Young et al. 2006 for Cas A in particular, Podsiadlowski et al. 1993, Woosley et al. 1994, Claeys et al. 2011, Dessart et al. 2012, Benvenuto et al. 2013, more generally). While SN 1987A was a Type II SN, the progenitor was also a blue rather than a red supergiant (see the review by Arnett et al. 1989). Several models have invoked binary interactions, possibly with a final merger, to explain either the structure of the star or the surrounding winds (e.g., Podsiadlowski & Joss 1989, Podsiadlowski 1992, Blondin & Lundqvist 1993, Morris & Podsiadlowski 2009).

Here we take advantage of the recently released PS1 survey data (PS1, hereafter, Chambers et al. 2016) along with their associated three-dimensional maps of dust in the Galaxy (Green et al. 2015) to examine stars near the centers of the Crab and Cas A quantitatively. For consistency with the dust maps, we use the extinction coefficients A_λ from Schlafly & Finkbeiner (2011). We also use, where available, the NOMAD (Zacharias et al. 2005) or HSOY (Altmann et al. 2017) proper motions. We fit the photome-

try of stars near the center of the SNR using Solar metallicity stars drawn from the PARSEC isochrones (Bressan et al. 2012). For the coarse luminosity estimates we require, the effects of metallicity on stellar colors should not be very important. For SN 1987A we simply examine the consequences of the new dust observations. In sections §2-4 we discuss the Crab, Cas A and SN 1987A in turn, and we discuss the implications of the results in §5.

2 THE CRAB (SN 1054)

Figure 1 shows the co-added grizy PS1 image of a roughly 2 arcmin region around the center of the Crab SNR. We adopt an age of 960 years and, following Kaplan et al. (2008), a distance of 2.0 ± 0.5 kpc or $\mu = 11.51 \pm 0.54$ as a distance modulus. Using the Green et al. (2015) dust distribution for the line of sight towards the center of the SNR, the extinction is roughly $E(B - V) \simeq 0.4$ mag. Green et al. (2015) estimate that the dust distribution is well-defined out to a distance modulus of 14.2 which is well beyond the distance to the Crab. This extinction estimate agrees well with other determinations (e.g., Wu 1981, Blair et al. 1992). We define the (J2000) center of the SNR as (05:34:32.84, 22:00:48.0) from Nugent (1998) and the position of the pulsar as (05:34:31.9, 22:00:52.1). Kaplan et al. (2008) measured the proper motion of the pulsar, and its estimated position at the time of the SN agrees very closely with the estimated center of the SNR. The center of the SNR and the position of the NS at present and in 1054 are both marked in Figure 1.

For a distance of 2.0 kpc and an age of 960 years, a star with velocity $v = 100v_2$ km/s has moved $10''.1v_2$. We selected stars within 1 arcmin of either the center of the SNR or the NS, corresponding to a velocity limit of approximately 600 km/s. Since the proper motion of the NS only corresponds to $v \simeq 100$ km/s and the Crab is believed to have been a Type II SN (even if peculiar) for which Equation 3 applies, only sources within roughly $10''.0$ of the center can plausibly be surviving secondaries.

The PS1 catalog for these 1 arcmin regions contains 171 sources, most of which are spurious detections created by the bright nebular emission or faint sources in the wings of the brighter point sources. When we went to fit models to the spectral energy distributions (SEDs) of the actual stars, we frequently found no good fits ($\chi^2 > 100$) for any stellar model even though we were using the PS1 PSF magnitudes. This is very different from the case of Cas A (next section), where we almost always found very good model fits. Presumably this is because the PS1 photometry pipeline was never intended for photometry of stars in a nebular emission region like the center of the Crab nebula. To remedy this issue, we used **SExtractor** (Bertin & Arnouts 1996) to identify sources on the roughly 2 arcmin square co-added PS1 image and then used **IRAF** aperture photometry with a 3 pixel ($0''.75$) aperture radius and a 6 pixel to 10 pixel radius sky aperture. This larger $2'$ area includes many stars beyond the brightest nebular regions. We then matched the aperture results to the PS1 photometry and computed the necessary photometric offsets as the median offset after clipping outliers. In the end we had 30 stars to consider, labeled in order of distance from the center of the SNR, including

the NS as star #5. Table 1 provides the positions and grizy aperture magnitudes of these 30 stars along with their distances from the center of the SNR and the NS.

There are, in fact, no sources closer than $12''.0$ to the center of the SNR. Since there is so little ambiguity in the center given its close (arcsecond) agreement with the proper motion of the pulsar, and even a $10''.0$ search radius is already generous for the companion of a Type II SN, we can immediately rule out the existence of a binary companion with $M_2 \gtrsim M_\odot$ simply from the structure of the CMD. This could be strengthened further using the still deeper HST data. There are six sources between $12''.0$ and $15''.0$, where the pulsar is source #5, and then the next source is $21''.7$ from the center. We number the sources by their distance from the center of the SNR and have labeled only the six closest sources in Figure 1.

Figure 2 shows the $r/r-i$ color magnitude diagram (CMD) of these sources. Superposed are the PARSEC isochrones for Solar metallicity stars with an age of $10^{7.3}$ years, roughly corresponding to the epoch at which $12M_\odot$ stars would die, along with the effects of changing the extinction estimates to $E(B - V) = 0$ or 0.9 mag. The distance uncertainties are much less important, since they only correspond to shifting the isochrone vertically by ± 0.5 mag. Like Guseinov et al. (2005), we find no plausible candidates for a former binary companion.

Seven of the stars (#1, 4, 13, 20, 21, 22 and 28) have proper motions in the NOMAD catalog, and their predicted positions at the time of the SN are indicated by the arrows in Figure 1. The uncertainties in the proper motions lead to a position uncertainty of approximately $12''.0$ after 960 years, as indicated by the circle at the end of one of the proper motion vectors. Only the distant star #22 has a proper motion consistent with the position of the SN, but it would also have to be moving at almost 600 km/s. The two closer stars with proper motions, #1 and #4, are moving in the wrong direction to be associated with the SN.

To formalize the qualitative impression, we drew a sample of roughly 10^5 stars from the PARSEC isochrones, uniformly sampling in age from 10^6 to 10^{10} years in increments of 0.01 dex. We fit the PARSEC estimates of the absolute PS1 magnitudes to all the candidate sources to estimate the distance and extinction. We considered four fits to each of the candidate sources for each of the $\sim 10^5$ stellar models. First, we fit for the extinction $E(B - V)$ and distance modulus μ with no constraints on either variable. Given magnitudes m_i with uncertainties σ_i and a model star with absolute magnitudes M_i , the fit statistic is

$$\chi_0^2 = \sum_i (m_i - M_i - \mu - R_i E(B - V))^2 \sigma_i^{-2}. \quad (4)$$

Second, we repeated the fits constrained by the estimated distance modulus $\mu_0 \pm \sigma_\mu$ to the Crab, $\chi_1^2 = \chi_0^2 + (\mu - \mu_0)^2 / \sigma_\mu^2$. For the last fit, we added a prior on the extinction based on the Green et al. (2015) estimates of the extinction as a function of distance modulus to the fit constrained by the distance modulus. We used the variance of their 20 alternate extinction realizations as an estimate of the uncertainty in the extinction at any given distance to give $E(\mu) \pm \sigma_{E(\mu)}$. We simply added this prior to the results of the previous fits to get $\chi_2^2 = \chi_1^2 + (E(B - V) - E(\mu))^2 / \sigma_{E(\mu)}^2$. We did not repeat the fits with the (non-linear) constraint on

the extinction as a function of distance – the broad range of the input models and the simplicity of the conclusions makes this complication unnecessary. We assumed uncertainties that are the larger of the photometric uncertainties and 0.05 mag. The minimum uncertainty is included to compensate for modest systematic errors (e.g., extinction law, photometric systems, calibrations, metallicity).

These fits are carried out for each of the $\sim 10^5$ stellar models, and the best fits are reported in Table 2. The table contains the goodness of fit for the best stellar model with no priors (χ_0^2), with a prior on the distance (χ_1^2), and with a prior on both the distance and the extinction (χ_2^2). In practice, there are reasonable fits for a range of stellar models, which we can characterize with quasi-Bayesian averages such as

$$\langle \log L \rangle = \left[\sum e^{-\chi'^2/2} \log L \right] \left[\sum e^{-\chi'^2/2} \right]^{-1} \quad (5)$$

for the luminosity. In these averages, χ'^2 means that we have renormalized the χ^2 values so that the best fit has a χ^2 per degree of freedom of unity if the raw χ^2 is larger than the number of degrees of freedom. This has the effect of broadening the uncertainties for sources which are less well fit. The same average is carried out for $\log T$. The allowed spreads of the luminosity and temperatures about the averages are estimated by the probability weighted dispersion of the solutions about the averages,

$$\sigma_{\log L}^2 = \left[\sum e^{-\chi'^2/2} (\log L - \langle \log L \rangle)^2 \right] \left[\sum e^{-\chi'^2/2} \right]^{-1}. \quad (6)$$

Table 2 reports these estimates of the luminosities and temperatures for the models with a prior on the distance but not on the extinction (χ_1^2) and the model with priors on both the extinction and the distance (χ_2^2).

As is typical of trying to estimate stellar distances using only photometry, it is nearly impossible to do so without additional constraints. Very few of the stars cannot be placed at the distance of the Crab if there is no constraint on the extinction (5 of 30 have $\chi_1^2 > \chi_0^2 + 4$). With the addition of the constraint on the extinction at any given distance included, many fewer have solutions consistent with the distance (15 of 30 have $\chi_2^2 > \chi_0^2 + 4$), but that still leaves many that are consistent with both priors. Curiously, the non-thermal emission of the NS (#5) can be well-modeled by a stellar SED.

Figure 3 shows the luminosities and temperatures the stars would have at the distance of the Crab and with the extinction prior (χ_2^2). The distribution looks similar without the extinction prior, but the uncertainties, particularly the temperature uncertainties, become larger (see Table 2). If any of these stars are at the distance of the Crab, none of them are either luminous or massive. Moreover, many of the more luminous stars are also the ones with proper motions, almost all of which are inconsistent with an association to SN 1054. More importantly, an actual companion to the Crab SN would have to be closer to the center of the SNR where no stars of similar magnitudes are observed. This implies that the Crab had no stellar companion to even stricter limits of $L \lesssim L_\odot$ and $M \lesssim M_\odot$ even if we are very conservative.

3 CASSIOPEIA A

Figure 4 shows the co-added grizy PS1 image of a roughly 2 arcmin region centered on Cas A. The emission lines present in some of the bands show an outline of the remnant, and we have marked the geometric center (23:23:27.82, 58:48:49.4) of the remnant (Thorstensen et al. 2001) and the position of the neutron star (23:23:27.93, 58:48:42.5). We adopt a distance of 3.4 ± 0.3 kpc (Reed et al. 1995) and an age of 330 years. For this distance, a source with velocity $100v_2$ km/s will have moved $2''0v_2$ in the 330 years since the SN. The $7''0$ distance of the NS from the center of the SNR corresponds to a velocity of approximately 340 km/s.

The PS1 extinction estimate at the distance of Cas A is $E(B - V) \simeq 1.2$ ($A_V = 3.7$) but it lies close to a sudden jump in the extinction to $E(B - V) \simeq 1.5$ ($A_V = 4.7$). This is more consistent with early estimates of $A_V \simeq 4.3$ mag by Searle (1971) and lower than the estimates of $A_V \simeq 5.3$ to 6.2 mag by Hurford & Fesen (1996) and $A_V = 6.2 \pm 0.6$ mag by Eriksen et al. (2009). These estimates are based on using predicted and observed SNR emission line ratios to determine the extinction. The distances used in the PS1 extinction estimates are only reliable out to Cas A.

We used a generous selection radius of $30''0$ from either the center of the SNR or the NS, which corresponds to a velocity of almost 1500 km/s. These regions contain 15 PS1 sources of which two are artifacts. This leaves thirteen stars, which we have again labeled in order of their distance from the center of the SNR as shown in Figure 4 and reported in Table 3. None of the stars have proper motion estimates in NOMAD and three (#4, #9 and #13) have proper motions in HSOY. The predicted positions of these three stars at the time of the SN are within a few arcseconds of their present positions and are too small to display in Figure 4. They cannot have been associated with the SN.

The closest star (#1) lies $11''.5$ from the center of the SNR and $16''.7$ from the NS, corresponding to velocities of 560 and 820 km/s that are not physical for the companion of a Type II (IIB) SN. The NS, while an X-ray source, is not detected to very deep optical/near-IR limits ($\gtrsim 28$ mag at R band, Fesen et al. 2006). We again replaced the PS1 magnitudes with the results of aperture photometry. Here nebula is not an issue and the PS1 PSF photometry produces good fits. However, replacing the PS1 PSF photometry with forced aperture aperture photometry allowed us to include photometry in more bands than PS1 reports due to limits on signal-to-noise ratios.

Figure 5 shows the z/i-z CMD of the stars. The brighter and closer (to the center) stars are labeled. Stars such as #4, #6 and #9 which could have $M > M_\odot$ at the distance of Cas A (and assuming more extinction than the PS1 model) are at least $24''0$ from the center or the NS and would require $v \gtrsim 1200$ km/s to be associated with the SN. Three of the four brightest stars (#4, #9 and #13) are also ruled out by their HSOY proper motions. There is no proper motion information for #6. The two closest PS1 stars would have to be $M \lesssim M_\odot$ and still require unreasonably high velocities.

Table 4 presents the results of fitting stellar models to the SEDs. Most of the stars can be well-fit, with star #5 as the worst case. We again find that roughly half the stars have properties consistent with the distance and extinction

of Cas A. Figure 6 shows the luminosities and temperatures of the stars including the extinction prior. As suggested by the CMD, stars #4, #6 and #9 can have the highest luminosities, with #4 potentially being a $\simeq 3M_{\odot}$ B star with $L \simeq 10^{2.0}L_{\odot}$. However, #4 and #9 also have HSOY proper motions inconsistent with any association. The rest of the stars would be low mass ($M < M_{\odot}$) dwarfs. As with the Crab, even these low mass stars are absent at distances from the center corresponding to reasonable velocities, so it is clear that any binary companion to Cas A at death would have to have $M \lesssim M_{\odot}$.

4 SN 1987A

Graves et al. (2005) obtained very tight limits on the presence of an optical point source at the center of SN 1987A, with limits of $\nu L_{\nu} < 0.26, 0.33, 0.15, 0.30$ and $0.28L_{\odot}$ in the F330W, F435W, F555W, F625W and F814W filters. To account for dust absorption in their estimates, they note that the fraction of the bolometric luminosity emerging in the infrared on day 2172 was 97% (Bouchet & Danziger 1993) implying an effective optical depth of $\tau \simeq 3.5$. The effective optical depth at the time their observations (day 6110) would then be $\tau = 0.45$ because of the $1/t^2$ dilution of the optical depth due to expansion. This then implies that there cannot be a binary companion (or other point source) more luminous than roughly $L < 2L_{\odot}$.

Graves et al. (2005) discuss scenarios in which the dust might be clumped, but these scenarios were based on clumpy dust distributions in a foreground screen rather than a circumstellar medium. For a clumpy medium closely surrounding the source, the extra absorption from a clump that happens to be along our line of sight will be partially balanced by the contribution from photons scattered onto our line of sight by other clumps (see the discussion in Kochanek et al. 2012). This would essentially eliminate the worst case scenario they consider, where there would be no dilution of the optical depth by expansion and the luminosity constraint would be ~ 30 times weaker.

A more important issue is that Herschel and ALMA observations imply the existence of $M_d \sim 0.5\text{--}1.0M_{\odot}$ of dust in SN 1987A (Matsuura et al. 2011, Indebetouw et al. 2014, Matsuura et al. 2015), far more than the amount inferred at early times as used by Graves et al. (2005). The characteristic visual optical depth scale for an SNR at time $t = 10t_{10}$ years is

$$\tau_0 = \frac{15\kappa M_d M_e}{64\pi E t^2} \simeq 30\kappa_4 M_{d0.1} M_{e10} E_{51}^{-1} t_{100}^{-2}. \quad (7)$$

where a typical dust visual opacity is $\kappa = 10^4 \kappa_4 \text{ cm}^2/\text{g}$, the dust mass is $M_d = 0.1M_{d0.1}M_{\odot}$, the total ejected mass is $M_e = 10M_{e10}M_{\odot}$ and the explosion energy is $E = 10^{51}E_{51} \text{ erg}$ (see Kochanek 2017). At $t = 16.7$ years (6110 days), the optical depth implied by the presently observed dust would have been $\tau_0 \sim 10\kappa_4 M_{d0.1} M_{e10} E_{51}^{-1}$ rather than the $\tau \simeq 0.5$ assumed by Graves et al. (2005). Even today, the optical depth would be of order $\tau_0 \sim 3\kappa_4 M_{d0.1} M_{e10} E_{51}^{-1}$. In short, given the amount of dust seen by Herschel and ALMA, the Graves et al. (2005) observations provide no useful limit on the luminosity of a binary companion (or emission from any stellar remnant).

As a result, it is really only the mid-IR dust emission which constrains the luminosity of any central source. Matsuura et al. (2015) find a total central dust luminosity in 2012 of $230L_{\odot}$. This luminosity is due to a combination of radioactive decay, absorption of radiation from the expanding shocks, and any contribution from a central source. Matsuura et al. (2015) estimate that the available heating from decay of ^{44}Ti is $\simeq 400L_{\odot}$, extrapolating from Jerkstrand et al. (2011), and that a further $\sim 50L_{\odot}$ can be heating from the shocks exterior to the dusty region. They do not discuss any additional contributions, but the two required heating sources already exceed the observed luminosity, which suggests that only a modest fraction of the observed $230L_{\odot}$ could be due to a binary companion. A reasonable upper limit is probably 10% of the total luminosity, which corresponds to $M \lesssim 2.5M_{\odot}$ (see Figure 6). A $3M_{\odot}$ companion would already represent half the observed luminosity.

5 DISCUSSION

Examining the PS1 sources near the Crab and Cas A, it is clear that these SN had no binary companion at death with a mass $M \gtrsim M_{\odot}$. Graves et al. (2005) found a similar limit for SN 1987A, but the higher present day estimates of the dust content imply a weaker limit of $M \lesssim 2.5M_{\odot}$ from the observed dust luminosity. In terms of mass ratios, there are no companions to these three ccSNe with initial mass ratios above $q \gtrsim 0.1$. If the binary fraction at death is f_b , the probability of finding no binaries companions in three systems is $(1 - f_b)^3$, implying that $f_b < 0.44$ at 90% confidence.

The stellar binary fraction of stars at death is generically lower than that at birth. Even for passively evolving binaries with no interactions, only the explosions of the primary are in a stellar binary. When the secondary explodes, the primary is a compact object which is likely both difficult to detect and need no longer be bound to the secondary. Following Equation 1 and again assuming a Salpeter IMF and a flat $P(q)$ distribution, the factor $f_q = 0.47$ if we detect all binaries with $q > 0.1$. This implies that the initial binary fraction is $F < 0.61$ at 90% confidence.

There is no simple way to estimate the initial binary fraction including binary interactions short of a full simulation of binary evolution, which is beyond our present scope. For example, the stars can merge, which would reduce the numbers of binaries at death. Alternatively, a primary with too little mass to explode can accrete enough mass from the secondary to explode, which would tend to increase the numbers of binaries at death. For example, if fraction f_M of binaries merge prior to the explosion of the primary, then we really have the limit $F(1 - f_M) < 0.61$. Sana et al. (2012) argue that $f_M \simeq 0.25$, which would shift the limit upwards to $F \lesssim 0.81$. In their review of binary populations, Duchêne & Kraus (2013) cite a multiplicity frequency (fraction of multiple systems) with $q > 0.1$ of $> 60\%$ and 80% for $8\text{--}16M_{\odot}$ and $> 16M_{\odot}$, respectively, while Moe & Di Stefano (2016) find that only $16 \pm 9\%$ ($6 \pm 6\%$) of $9\text{--}16M_{\odot}$ ($> 16M_{\odot}$) primaries are single. Thus, if there are only singles or binaries, the binary fractions can be reconciled by a having a significant merger fraction.

However, many massive stars are in higher order systems (triples, etc.), and this reintroduces the tension. The fraction of massive stars in higher order systems is high – Moe & Di Stefano (2016) find that $(52 \pm 13)\%$ ($73 \pm 16\%$) of $9-16M_{\odot}$ ($> 16M_{\odot}$) primaries are in higher order systems with $q > 0.1$. Let $f_H \simeq 62\%$ be the fraction of non-single stars in higher order systems (i.e. 32% are in binaries and 52% are in higher order systems, and $62 = 52/(52 + 32)$). The fraction of exploding primaries is still $f_p = F/(1 + Ff_q)$ where F is now the fraction of non-single stars at birth. The fraction of these with a stellar secondary and no additional companion is $(1 - f_H)(1 - f_M)$ where we allow fraction f_M of binaries to merge. The fraction where there is an additional companion, so that there is a stellar companion independent of whether the primary and secondary have merged, is f_H . Thus, the fraction of exploding primaries with a stellar companion (not necessarily the original secondary) is reduced by $(1 - f_H)(1 - f_M) + f_H \simeq 91\%$ rather than $1 - f_M \simeq 75\%$ for $f_H = 62\%$ and a merger fraction of $f_M = 25\%$. Accounting for these higher order systems, the limit on the initial fraction of non-single stars is $F(1 - f_M + f_H f_M) < 0.61$, leading to a limit of $F \lesssim 0.67$ that is again in significant tension with estimates of stellar multiplicities.

This ignores any contribution from secondaries exploding in higher order systems which survive the explosion of the primary. The fraction of exploding secondaries in this passive evolution model is $f_s = Ff_q/(1 + Ff_q) \simeq 26\%$ for $f_q = 0.47$ and $F = 0.75$. In the absence of higher order systems, none of these would have stellar companions at death since the primary becomes a compact object independent of whether the binary survives. With higher order systems, fraction f_H of the explosions of secondaries could also have a stellar companion at death, although probably only a small fraction of these systems remain bound following the explosion of the primary.

A second interesting point is that Cas A was a Type IIb SN (Krause et al. 2008, Rest et al. 2008) and yet it cannot have been a binary at death unless the companion was a dwarf star or a compact object. Many models for Type IIb SN invoke binary evolution and a massive companion, as was originally suggested by Podsiadlowski et al. (1993) and Woosley et al. (1994) to explain SN 1993J. Searches for an optical counterpart to the Cas A NS noted that any bound binary companion would have to be very low mass (e.g., Chakrabarty et al. 2001, Fesen et al. 2006), but we could find no quantitative discussion of limits on unbound binary companions. Cas A is one of the SNR without candidate O/B star companions in Guseinov et al. (2005) and the issue is mentioned in passing by Claeys et al. (2011). In their survey of possible binary models for Type IIb SNe, Claeys et al. (2011) essentially always were left with a companion that should have been easily visible. This suggests that caution should be exercised about invoking this theoretical motivation in searches for companions to other Type IIb SNe like SN 1993J (e.g., Maund et al. 2004, Fox et al. 2014) or SN 2011dh (e.g., Folatelli et al. 2014, Maund et al. 2015).

That the absence of binary companions in only three systems already has interesting implications suggests greatly expanding such searches. The expected rate of companions is so high that it already surprising not to have found one in these three systems, so even doubling the sample should either yield an example or indicate a serious problem – with

six systems and no detection $f_b < 28\%$ at 90% confidence. The three systems we consider here are a peculiar if well-defined sample, and it is not clear how to incorporate the possible detection in SNR S147 (Dingel et al. 2015). If we simply treat it like a sample of four objects with one detection, then $f_b \simeq 31\%$ with a symmetric 90% confidence range of $8\% < f_b < 66\%$ that leaves much of tension intact.

The Crab and Cas A are the easiest Galactic systems to examine due to their youth and low extinction and stellar densities. Searches to binary companions of ccSNe are intrinsically easier than those for Type Ia because there is no immediate need to rule out the existence of faint, dwarf companions. The searches should probably not be limited to O/B stars (as in Guseinov et al. 2005). For passively evolving binaries, companions will be dominated by main sequence stars (Kochanek 2009), but binary evolution and mass transfer greatly broadens the spectrum of possible secondaries. It is necessary to separate the ccSNe from the Type Ia's using the presence of a NS, the composition/structure of the SNR (e.g., Lopez et al. 2009, Yamaguchi et al. 2014), or, as done for Cas A, light echo spectra. Modern, multiband photometry such as the PS1 data used here, is an important improvement, but studying large numbers of additional Galactic SNRs will only become relatively straight forward with the release of the full Gaia proper motion and parallax catalogs (e.g., Gaia Collaboration et al. 2016). Searching SNRs in the Magellanic Clouds is also feasible starting from catalogs like Harris & Zaritsky (2004) or Nidever et al. (2017). While proper motions will be lacking, the fixed distance and modest extinctions otherwise simplify the problem.

Identifying these binary companions to ccSNe is important. Not only are they a key observational constraint on the role of binaries in ccSNe, but they also provide important constraints on the formation of runaway stars and the origins of NS velocities. For example, having the velocity of the former binary companion would greatly help to separate the contributions of binary disruption and explosive kicks to the velocities of NS. It would also be interesting to identify such systems to observe the consequences of the SN explosion for the secondary. This has primarily been considered for stellar companions to Type Ia SN (e.g., Marietta et al. 2000, Shappee et al. 2013, Pan et al. 2014), but there should also be long term effects on close companions to ccSNe.

ACKNOWLEDGMENTS

CSK thanks K. Auchettl, C. Badenes, S. de Mink, J. J. Eldridge, T. Holland-Ashford, L. Lopez, K. Stanek, M. Pinsonneault, and T. Thompson for discussions and comments. CSK is supported by NSF grants AST-1515876 and AST-1515927.

REFERENCES

- Altmann, M., Roeser, S., Demleitner, M., Bastian, U., & Schilbach, E. 2017, arXiv:1701.02629
- Arnett, W. D., Bahcall, J. N., Kirshner, R. P., & Woosley, S. E. 1989, ARA&A, 27, 629

Table 1. Stars Near the Crab

| # | d_c | d_{NS} | RA | Dec | g | r | i | z | y |
|----|-------|----------|-----------|-----------|--------------------|--------------------|--------------------|--------------------|--------------------|
| 1 | 12''1 | 10''8 | 83.633751 | 22.011540 | 17.875 \pm 0.007 | 16.749 \pm 0.005 | 16.508 \pm 0.005 | 16.232 \pm 0.005 | 16.098 \pm 0.005 |
| 2 | 12''2 | 5''6 | 83.634080 | 22.015580 | 16.406 \pm 0.005 | 15.429 \pm 0.004 | 15.102 \pm 0.004 | 14.941 \pm 0.003 | 14.875 \pm 0.004 |
| 3 | 13''2 | 5''6 | 83.632910 | 22.012900 | 20.213 \pm 0.041 | 18.479 \pm 0.018 | 17.886 \pm 0.017 | 17.490 \pm 0.009 | 17.114 \pm 0.011 |
| 4 | 13''2 | 22''0 | 83.639220 | 22.016270 | 17.145 \pm 0.005 | 16.076 \pm 0.004 | 15.767 \pm 0.003 | 15.870 \pm 0.005 | 15.513 \pm 0.004 |
| 5 | 13''4 | 0''5 | 83.633031 | 22.014530 | 17.207 \pm 0.009 | 16.304 \pm 0.009 | 16.088 \pm 0.009 | 15.821 \pm 0.007 | 15.687 \pm 0.009 |
| 6 | 14''2 | 12''4 | 83.633381 | 22.011031 | 18.836 \pm 0.011 | 17.822 \pm 0.011 | 17.578 \pm 0.009 | 17.343 \pm 0.009 | 17.163 \pm 0.011 |
| 7 | 21''6 | 32''2 | 83.642270 | 22.016590 | 21.955 \pm 0.330 | 20.354 \pm 0.110 | 18.801 \pm 0.029 | 18.147 \pm 0.021 | 17.785 \pm 0.025 |
| 8 | 28''0 | 41''3 | 83.643901 | 22.009151 | 21.057 \pm 0.118 | 19.822 \pm 0.053 | 19.412 \pm 0.050 | 19.336 \pm 0.057 | 19.104 \pm 0.099 |
| 9 | 29''1 | 31''3 | 83.633680 | 22.005790 | 22.833 \pm 0.327 | 20.526 \pm 0.067 | 19.380 \pm 0.044 | 19.003 \pm 0.030 | 18.544 \pm 0.035 |
| 10 | 30''3 | 43''4 | 83.644091 | 22.008290 | 19.849 \pm 0.030 | 18.572 \pm 0.026 | 18.195 \pm 0.013 | 18.019 \pm 0.013 | 17.729 \pm 0.022 |
| 11 | 31''3 | 24''3 | 83.632790 | 22.021190 | 18.055 \pm 0.009 | 16.971 \pm 0.005 | 16.813 \pm 0.009 | 16.396 \pm 0.005 | 16.398 \pm 0.007 |
| 12 | 32''9 | 24''8 | 83.627980 | 22.009300 | 20.487 \pm 0.066 | 19.226 \pm 0.026 | 18.745 \pm 0.019 | 18.357 \pm 0.018 | 18.355 \pm 0.059 |
| 13 | 40''1 | 53''7 | 83.648400 | 22.010360 | 15.976 \pm 0.004 | 14.929 \pm 0.003 | 14.580 \pm 0.003 | 14.377 \pm 0.002 | 14.258 \pm 0.003 |
| 14 | 42''1 | 45''7 | 83.634560 | 22.001831 | 21.708 \pm 0.131 | 20.549 \pm 0.103 | 21.173 \pm 0.168 | 21.441 \pm 0.346 | 20.392 \pm 0.264 |
| 15 | 43''8 | 57''1 | 83.649970 | 22.013350 | 19.691 \pm 0.019 | 18.806 \pm 0.025 | 18.246 \pm 0.011 | 18.137 \pm 0.015 | 17.996 \pm 0.030 |
| 16 | 44''3 | 56''2 | 83.645360 | 22.003920 | 19.306 \pm 0.025 | 17.970 \pm 0.018 | 17.516 \pm 0.009 | 17.264 \pm 0.013 | 17.008 \pm 0.018 |
| 17 | 44''5 | 31''4 | 83.623531 | 22.014000 | 21.403 \pm 0.155 | 19.944 \pm 0.095 | 19.034 \pm 0.046 | 18.747 \pm 0.054 | 18.441 \pm 0.064 |
| 18 | 46''3 | 36''4 | 83.623841 | 22.008830 | 19.301 \pm 0.043 | 18.178 \pm 0.028 | 17.915 \pm 0.022 | 17.711 \pm 0.013 | 17.572 \pm 0.028 |
| 19 | 52''5 | 47''0 | 83.633171 | 22.027510 | 21.674 \pm 0.130 | 19.710 \pm 0.029 | 18.614 \pm 0.024 | 18.098 \pm 0.017 | 17.837 \pm 0.021 |
| 20 | 53''9 | 67''1 | 83.652970 | 22.013090 | 18.549 \pm 0.013 | 17.471 \pm 0.011 | 16.953 \pm 0.009 | 16.819 \pm 0.009 | 16.612 \pm 0.013 |
| 21 | 54''1 | 63''6 | 83.642910 | 21.999390 | 17.840 \pm 0.011 | 16.788 \pm 0.011 | 16.540 \pm 0.007 | 16.369 \pm 0.005 | 16.098 \pm 0.009 |
| 22 | 56''5 | 62''2 | 83.637380 | 21.997660 | 16.915 \pm 0.005 | 15.841 \pm 0.004 | 15.490 \pm 0.005 | 15.354 \pm 0.004 | 15.119 \pm 0.005 |
| 23 | 56''7 | 45''2 | 83.625051 | 22.024660 | 21.395 \pm 0.129 | 20.314 \pm 0.137 | 19.727 \pm 0.071 | 19.585 \pm 0.075 | 19.326 \pm 0.088 |
| 24 | 58''8 | 72''4 | 83.653070 | 22.007001 | 19.107 \pm 0.013 | 17.892 \pm 0.007 | 17.595 \pm 0.009 | 17.162 \pm 0.007 | 17.182 \pm 0.015 |
| 25 | 59''3 | 72''2 | 83.650590 | 22.002890 | 20.473 \pm 0.041 | 19.430 \pm 0.040 | 19.089 \pm 0.036 | 18.953 \pm 0.036 | 18.766 \pm 0.054 |
| 26 | 60''6 | 53''2 | 83.621881 | 22.003800 | 19.146 \pm 0.015 | 18.085 \pm 0.009 | 17.933 \pm 0.009 | 17.620 \pm 0.009 | 17.480 \pm 0.013 |
| 27 | 63''8 | 50''2 | 83.618310 | 22.017740 | 19.334 \pm 0.018 | 18.261 \pm 0.026 | 17.996 \pm 0.015 | 17.825 \pm 0.015 | 17.564 \pm 0.021 |
| 28 | 66''5 | 55''4 | 83.617581 | 22.008580 | 17.723 \pm 0.007 | 16.672 \pm 0.005 | 16.724 \pm 0.007 | 16.229 \pm 0.005 | 16.051 \pm 0.007 |
| 29 | 68''1 | 55''2 | 83.620091 | 22.024130 | 21.746 \pm 0.236 | 19.173 \pm 0.086 | 18.695 \pm 0.018 | 18.258 \pm 0.015 | 17.765 \pm 0.030 |
| 30 | 68''3 | 55''9 | 83.616450 | 22.011591 | 18.793 \pm 0.017 | 18.011 \pm 0.018 | 17.899 \pm 0.011 | 17.694 \pm 0.009 | 17.448 \pm 0.017 |

The stars are numbered in order of their distance from the center of the SNR (d_c) and the distance from the NS (d_{NS}) is also given. The magnitudes are aperture magnitudes found from the PS1 images and an entry of – indicates no detection.

Benvenuto, O. G., Bersten, M. C., & Nomoto, K. 2013, *ApJ*, 762, 74
 Bersten, M. C., Benvenuto, O. G., Folatelli, G., et al. 2014, *AJ*, 148, 68
 Bertin, E., & Arnouts, S. 1996, *A&AS*, 117, 393
 Blaauw, A. 1961, *BAIN*, 15, 265
 Blair, W. P., Long, K. S., Vancura, O., et al. 1992, *ApJ*, 399, 611
 Blondin, J. M., & Lundqvist, P. 1993, *ApJ*, 405, 337
 Bouchet, P., & Danziger, I. J. 1993, *AAP*, 273, 451
 Bressan, A., Marigo, P., Girardi, L., et al. 2012, *MNRAS*, 427, 127
 Cao, Y., Kasliwal, M. M., Arcavi, I., et al. 2013, *ApJL*, 775, L7
 Chakrabarty, D., Pivovarov, M. J., Hernquist, L. E., Heyl, J. S., & Narayan, R. 2001, *ApJ*, 548, 800
 Chambers, K. C., Magnier, E. A., Metcalfe, N., et al. 2016, *arXiv:1612.05560*
 Claeys, J. S. W., de Mink, S. E., Pols, O. R., Eldridge, J. J., & Baes, M. 2011, *AAP*, 528, A131
 Cordes, J. M., & Chernoff, D. F. 1998, *ApJ*, 505, 315
 Crockett, R. M., Smartt, S. J., Eldridge, J. J., et al. 2007, *MNRAS*, 381, 835
 Crockett, R. M., Eldridge, J. J., Smartt, S. J., et al. 2008, *MNRAS*, 391, L5
 De Donder, E., & Vanbeveren, D. 1998, *AAP*, 333, 557
 Dessart, L., Hillier, D. J., Li, C., & Woosley, S. 2012, *MN-*

RAS, 424, 2139
 Dinçel, B., Neuhäuser, R., Yerli, S. K., et al. 2015, *MNRAS*, 448, 3196
 Duchêne, G., & Kraus, A. 2013, *ARA&A*, 51, 269
 Eldridge, J. J., Izzard, R. G., & Tout, C. A. 2008, *MNRAS*, 384, 1109
 Eldridge, J. J., Langer, N., & Tout, C. A. 2011, *MNRAS*, 414, 3501
 Eldridge, J. J., Fraser, M., Smartt, S. J., Maund, J. R., & Crockett, R. M. 2013, *MNRAS*, 436, 774
 Eldridge, J. J., Fraser, M., Maund, J. R., & Smartt, S. J. 2015, *MNRAS*, 446, 2689
 Eldridge, J. J., & Maund, J. R. 2016, *MNRAS*, 461, L117
 Eriksen, K. A., Arnett, D., McCarthy, D. W., & Young, P. 2009, *ApJ*, 697, 29
 Faucher-Giguère, C.-A., & Kaspi, V. M. 2006, *ApJ*, 643, 332
 Fesen, R. A., Pavlov, G. G., & Sanwal, D. 2006, *ApJ*, 636, 848
 Finn, K., Bianco, F. B., Modjaz, M., Liu, Y.-Q., & Rest, A. 2016, *ApJ*, 830, 73
 Folatelli, G., Bersten, M. C., Benvenuto, O. G., et al. 2014, *ApJL*, 793, L22
 Folatelli, G., Van Dyk, S. D., Kuncarayakti, H., et al. 2016, *ApJL*, 825, L22
 Fox, O. D., Azalee Bostroem, K., Van Dyk, S. D., et al. 2014, *ApJ*, 790, 17

Table 2. Fits to Stars Near the Crab

| # | χ_0^2 | χ_1^2 | χ_2^2 | $\log L_1/L_\odot$ | $\log T_1$ | $\log L_2/L_\odot$ | $\log T_2$ |
|----|------------|------------|------------|--------------------|-------------------|--------------------|-------------------|
| 1 | 5.5 | 6.0 | 8.1 | 0.06 ± 0.25 | 3.672 ± 0.030 | 0.17 ± 0.30 | 3.711 ± 0.004 |
| 2 | 0.1 | 0.9 | 3.9 | 0.44 ± 0.24 | 3.681 ± 0.024 | 0.67 ± 0.20 | 3.736 ± 0.004 |
| 3 | 9.8 | 10.3 | 26.6 | -0.11 ± 0.33 | 3.676 ± 0.037 | -0.65 ± 0.47 | 3.602 ± 0.005 |
| 4 | 21.9 | 23.6 | 30.7 | 0.28 ± 0.48 | 3.716 ± 0.074 | 0.27 ± 0.49 | 3.740 ± 0.009 |
| 5 | 3.6 | 5.6 | 5.7 | 0.40 ± 0.32 | 3.764 ± 0.067 | 0.35 ± 0.26 | 3.745 ± 0.004 |
| 6 | 24.9 | 30.9 | 31.0 | 0.04 ± 0.55 | 3.748 ± 0.077 | -0.17 ± 0.28 | 3.730 ± 0.008 |
| 7 | 0.1 | 0.5 | 0.7 | -0.57 ± 0.23 | 3.545 ± 0.021 | -0.67 ± 0.19 | 3.533 ± 0.003 |
| 8 | 5.1 | 9.5 | 16.7 | -0.71 ± 0.17 | 3.659 ± 0.021 | -0.37 ± 0.12 | 3.716 ± 0.008 |
| 9 | 13.5 | 14.3 | 17.8 | -0.41 ± 0.47 | 3.686 ± 0.069 | -0.97 ± 0.35 | 3.566 ± 0.004 |
| 10 | 17.8 | 19.2 | 19.9 | -0.41 ± 0.37 | 3.688 ± 0.046 | -0.50 ± 0.24 | 3.681 ± 0.005 |
| 11 | 12.7 | 15.0 | 16.8 | 0.04 ± 0.39 | 3.709 ± 0.057 | -0.04 ± 0.38 | 3.721 ± 0.006 |
| 12 | 8.2 | 10.1 | 10.5 | -0.62 ± 0.30 | 3.666 ± 0.040 | -0.61 ± 0.16 | 3.668 ± 0.003 |
| 13 | 0.5 | 1.8 | 2.5 | 0.81 ± 0.23 | 3.703 ± 0.020 | 0.82 ± 0.18 | 3.712 ± 0.003 |
| 14 | 26.1 | 54.1 | 79.9 | -0.29 ± 0.42 | 3.714 ± 0.052 | 0.05 ± 0.22 | 3.762 ± 0.016 |
| 15 | 8.7 | 10.0 | 11.5 | -0.37 ± 0.32 | 3.706 ± 0.045 | -0.36 ± 0.11 | 3.715 ± 0.004 |
| 16 | 3.6 | 3.8 | 3.9 | -0.25 ± 0.23 | 3.667 ± 0.025 | -0.23 ± 0.24 | 3.662 ± 0.002 |
| 17 | 6.9 | 7.1 | 7.4 | -0.71 ± 0.38 | 3.650 ± 0.055 | -0.93 ± 0.14 | 3.610 ± 0.002 |
| 18 | 15.6 | 18.0 | 21.1 | -0.40 ± 0.35 | 3.691 ± 0.043 | -0.29 ± 0.19 | 3.719 ± 0.006 |
| 19 | 23.6 | 27.6 | 32.8 | 0.04 ± 0.64 | 3.736 ± 0.096 | -0.83 ± 0.40 | 3.564 ± 0.006 |
| 20 | 1.9 | 1.9 | 2.1 | -0.11 ± 0.25 | 3.685 ± 0.051 | -0.06 ± 0.23 | 3.691 ± 0.003 |
| 21 | 9.1 | 9.5 | 10.9 | 0.12 ± 0.35 | 3.716 ± 0.063 | 0.05 ± 0.36 | 3.722 ± 0.005 |
| 22 | 3.7 | 4.3 | 5.7 | 0.39 ± 0.23 | 3.682 ± 0.027 | 0.56 ± 0.21 | 3.710 ± 0.003 |
| 23 | 2.0 | 4.9 | 8.4 | -0.89 ± 0.19 | 3.629 ± 0.024 | -0.63 ± 0.08 | 3.676 ± 0.003 |
| 24 | 8.2 | 11.9 | 12.6 | -0.29 ± 0.34 | 3.686 ± 0.044 | -0.32 ± 0.31 | 3.689 ± 0.005 |
| 25 | 3.2 | 6.0 | 12.4 | -0.70 ± 0.16 | 3.662 ± 0.019 | -0.29 ± 0.11 | 3.726 ± 0.007 |
| 26 | 22.3 | 26.1 | 27.4 | -0.18 ± 0.46 | 3.720 ± 0.059 | -0.20 ± 0.22 | 3.731 ± 0.007 |
| 27 | 17.7 | 20.3 | 21.6 | -0.29 ± 0.40 | 3.709 ± 0.051 | -0.28 ± 0.20 | 3.721 ± 0.007 |
| 28 | 37.2 | 46.4 | 46.9 | 0.70 ± 0.78 | 3.828 ± 0.135 | 0.15 ± 0.50 | 3.736 ± 0.012 |
| 29 | 28.3 | 28.6 | 45.2 | 0.04 ± 0.59 | 3.737 ± 0.088 | -0.87 ± 0.42 | 3.592 ± 0.004 |
| 30 | 18.1 | 27.5 | 29.9 | 0.07 ± 0.54 | 3.765 ± 0.071 | 0.22 ± 0.20 | 3.785 ± 0.011 |

The ID numbers are the same as in Table 1. The goodnesses of fit χ_0^2 , χ_1^2 , and χ_2^2 are for fits with no prior, a prior for the distance to the SN, and a prior on both the distance and the extinction. The probability weighted mean luminosities and temperatures are reported for the latter two models.

Table 3. Stars Near Cas A

| # | d_c | d_{NS} | RA | Dec | g | r | i | z | y |
|----|-------|----------|------------|-----------|--------------------|--------------------|--------------------|--------------------|--------------------|
| 1 | 11''7 | 16''9 | 350.869920 | 58.816130 | 26.968 ± 6.896 | 22.959 ± 0.243 | 21.610 ± 0.085 | 21.066 ± 0.096 | 20.460 ± 0.127 |
| 2 | 16''6 | 21''9 | 350.871040 | 58.817400 | 24.223 ± 0.478 | 22.431 ± 0.153 | 21.512 ± 0.089 | 20.907 ± 0.093 | 20.540 ± 0.143 |
| 3 | 19''8 | 26''7 | 350.862510 | 58.818970 | — | 23.087 ± 0.241 | 21.694 ± 0.102 | 20.755 ± 0.072 | 20.069 ± 0.086 |
| 4 | 23''8 | 25''3 | 350.853010 | 58.813060 | 16.802 ± 0.003 | 15.775 ± 0.003 | 15.306 ± 0.003 | 14.939 ± 0.003 | 14.712 ± 0.003 |
| 5 | 25''3 | 32''2 | 350.861801 | 58.820450 | 23.675 ± 0.290 | 22.005 ± 0.119 | 20.701 ± 0.051 | 20.375 ± 0.051 | 19.764 ± 0.066 |
| 6 | 28''0 | 32''9 | 350.852650 | 58.817580 | 19.784 ± 0.009 | 18.349 ± 0.007 | 17.633 ± 0.005 | 17.278 ± 0.007 | 17.003 ± 0.009 |
| 7 | 28''3 | 24''7 | 350.855350 | 58.807990 | 26.995 ± 4.898 | 23.297 ± 0.335 | 22.169 ± 0.126 | 21.046 ± 0.096 | 20.221 ± 0.110 |
| 8 | 28''5 | 32''6 | 350.851430 | 58.816520 | 24.604 ± 0.551 | 22.601 ± 0.194 | 21.244 ± 0.066 | 20.224 ± 0.050 | 19.396 ± 0.046 |
| 9 | 28''5 | 22''0 | 350.863360 | 58.805910 | 18.290 ± 0.004 | 17.258 ± 0.004 | 16.596 ± 0.003 | 16.304 ± 0.004 | 16.072 ± 0.004 |
| 10 | 29''6 | 23''1 | 350.873351 | 58.806511 | 23.511 ± 0.237 | 21.663 ± 0.069 | 20.273 ± 0.026 | 19.595 ± 0.018 | 19.317 ± 0.038 |
| 11 | 32''4 | 27''1 | 350.878290 | 58.807510 | 24.849 ± 0.694 | 22.528 ± 0.179 | 21.322 ± 0.074 | 20.694 ± 0.062 | 20.674 ± 0.186 |
| 12 | 34''9 | 29''4 | 350.878871 | 58.806840 | 23.770 ± 0.284 | 22.723 ± 0.270 | 20.867 ± 0.043 | 20.308 ± 0.042 | 19.909 ± 0.076 |
| 13 | 35''5 | 29''2 | 350.861641 | 58.804091 | 20.880 ± 0.018 | 19.655 ± 0.011 | 18.956 ± 0.007 | 18.598 ± 0.011 | 18.278 ± 0.015 |

The stars are numbered in order of their distance from the center of the SNR (d_c) and the distance from the NS (d_{NS}) is also given. The magnitudes are aperture magnitudes found from the PS1 images and an entry of — indicates no detection.

Fremling, C., Sollerman, J., Taddia, F., et al. 2014, AAP, 565, A114

Gaia Collaboration, Brown, A. G. A., Vallenari, A., et al. 2016, AAP, 595, A2

Gies, D. R., & Bolton, C. T. 1986, ApJS, 61, 419

González Hernández, J. I., Ruiz-Lapuente, P., Tabernero, H. M., et al. 2012, Nature, 489, 533

Graves, G. J. M., Challis, P. M., Chevalier, R. A., et al. 2005, ApJ, 629, 944

Green, D. A. 2014, Bulletin of the Astronomical Society of India, 42, 47

Green, G. M., Schlafly, E. F., Finkbeiner, D. P., et al. 2015, ApJ, 810, 25

Groh, J. H., Georgy, C., & Ekström, S. 2013, AAP, 558, L1

Table 4. Fits to Stars Near Cas A

| # | χ_0^2 | χ_1^2 | χ_2^2 | $\log L_1/L_\odot$ | $\log T_1$ | $\log L_2/L_\odot$ | $\log T_2$ |
|----|------------|------------|------------|--------------------|-------------------|--------------------|-------------------|
| 1 | 1.5 | 2.0 | 2.1 | -0.81 ± 0.30 | 3.635 ± 0.052 | -0.91 ± 0.12 | 3.619 ± 0.010 |
| 2 | 0.2 | 1.3 | 3.2 | -1.08 ± 0.25 | 3.598 ± 0.032 | -0.70 ± 0.12 | 3.664 ± 0.013 |
| 3 | 0.7 | 2.2 | 5.9 | -0.07 ± 0.22 | 3.738 ± 0.051 | -0.75 ± 0.14 | 3.547 ± 0.009 |
| 4 | 0.6 | 1.5 | 1.6 | 2.26 ± 0.50 | 4.074 ± 0.152 | 2.04 ± 0.48 | 3.992 ± 0.131 |
| 5 | 15.3 | 17.4 | 17.6 | -0.61 ± 0.33 | 3.660 ± 0.062 | -0.53 ± 0.23 | 3.684 ± 0.032 |
| 6 | 0.3 | 0.4 | 1.8 | 0.44 ± 0.17 | 3.703 ± 0.041 | 0.57 ± 0.16 | 3.768 ± 0.030 |
| 7 | 3.2 | 5.7 | 10.9 | -0.00 ± 0.28 | 3.741 ± 0.061 | -0.85 ± 0.16 | 3.522 ± 0.014 |
| 8 | 8.7 | 16.4 | 30.6 | 0.50 ± 0.37 | 3.806 ± 0.076 | -0.59 ± 0.21 | 3.526 ± 0.021 |
| 9 | 0.2 | 0.8 | 0.9 | 1.28 ± 0.34 | 3.913 ± 0.094 | 1.26 ± 0.32 | 3.906 ± 0.072 |
| 10 | 2.9 | 3.6 | 7.6 | -0.65 ± 0.15 | 3.558 ± 0.014 | -0.36 ± 0.17 | 3.619 ± 0.015 |
| 11 | 2.8 | 3.4 | 4.1 | -0.93 ± 0.29 | 3.614 ± 0.048 | -0.78 ± 0.13 | 3.645 ± 0.013 |
| 12 | 2.3 | 3.7 | 9.5 | -1.06 ± 0.17 | 3.523 ± 0.027 | -0.60 ± 0.21 | 3.659 ± 0.031 |
| 13 | 4.1 | 7.2 | 9.4 | 0.06 ± 0.17 | 3.770 ± 0.022 | -0.04 ± 0.13 | 3.761 ± 0.011 |

The ID numbers are the same as in Table 3. The goodnesses of fit χ_0^2 , χ_1^2 , and χ_2^2 are for fits with no prior, a prior for the distance to the SN, and a prior on both the distance and the extinction. The probability weighted mean luminosities and temperatures are reported for the latter two models.

- Gunn, J. E., & Ostriker, J. P. 1970, *ApJ*, 160, 979
- Guseinov, O. H., Ankay, A., & Tagieva, S. O. 2005, *Astrophysics*, 48, 330
- Harris, J., & Zaritsky, D. 2004, *AJ*, 127, 1531
- Hester, J. J. 2008, *ARA&A*, 46, 127
- Hoogerwerf, R., de Bruijne, J. H. J., & de Zeeuw, P. T. 2001, *AAP*, 365, 49
- Hurford, A. P., & Fesen, R. A. 1996, *ApJ*, 469, 246
- Iben, I., Jr., & Tutukov, A. V. 1996, *ApJ*, 456, 738
- Ihara, Y., Ozaki, J., Doi, M., et al. 2007, *PASJ*, 59, 811
- Indebetouw, R., Matsuura, M., Dwek, E., et al. 2014, *ApJL*, 782, L2
- Jerkstrand, A., Fransson, C., & Kozma, C. 2011, *AAP*, 530, A45
- Kaplan, D. L., Kulkarni, S. R., & Murray, S. S. 2001, *ApJ*, 558, 270
- Kaplan, D. L., Chatterjee, S., Gaensler, B. M., & Anderson, J. 2008, *ApJ*, 677, 1201-1215
- Kim, H.-J., Yoon, S.-C., & Koo, B.-C. 2015, *ApJ*, 809, 131
- Kobulnicky, H. A., Kiminki, D. C., Lundquist, M. J., et al. 2014, *ApJS*, 213, 34
- Kochanek, C. S. 2009, *ApJ*, 707, 1578
- Kochanek, C. S., Khan, R., & Dai, X. 2012, *ApJ*, 759, 20
- Kochanek, C. S., 2017, in preparation
- Krause, O., Birkmann, S. M., Usuda, T., et al. 2008, *Science*, 320, 1195
- Li, W., Van Dyk, S. D., Filippenko, A. V., et al. 2006, *ApJ*, 641, 1060
- Lopez, L. A., Ramirez-Ruiz, E., Badenes, C., et al. 2009, *ApJL*, 706, L106
- Marietta, E., Burrows, A., & Fryxell, B. 2000, *ApJS*, 128, 615
- Matsuura, M., Dwek, E., Meixner, M., et al. 2011, *Science*, 333, 1258
- Matsuura, M., Dwek, E., Barlow, M. J., et al. 2015, *ApJ*, 800, 50
- Mattila, S., Smartt, S. J., Eldridge, J. J., et al. 2008, *ApJL*, 688, L91
- Maund, J. R., Smartt, S. J., Kudritzki, R. P., Podsiadlowski, P., & Gilmore, G. F. 2004, *Nature*, 427, 129
- Maund, J. R., Smartt, S. J., & Danziger, I. J. 2005, *MNRAS*, 364, L33
- Maund, J. R., Arcavi, I., Ergon, M., et al. 2015, *MNRAS*, 454, 2580
- Moe, M., & Di Stefano, R. 2016, *arXiv:1606.05347*
- Monet, D., Canzian, B., Harris, H., et al. 1998, *VizieR Online Data Catalog*, 1243
- Moriya, T. J., & Eldridge, J. J. 2016, *MNRAS*, 461, 2155
- Morris, T., & Podsiadlowski, P. 2009, *MNRAS*, 399, 515
- Nidever, D. L., Olsen, K., Walker, A. R., et al. 2017, *arXiv:1701.00502*
- Nugent, R. L. 1998, *PASP*, 110, 831
- Pan, K.-C., Ricker, P. M., & Taam, R. E. 2014, *ApJ*, 792, 71
- Podsiadlowski, P., & Joss, P. C. 1989, *Nature*, 338, 401
- Podsiadlowski, P. 1992, *PASP*, 104, 717
- Podsiadlowski, P., Hsu, J. J. L., Joss, P. C., & Ross, R. R. 1993, *Nature*, 364, 509
- Reed, J. E., Hester, J. J., Fabian, A. C., & Winkler, P. F. 1995, *ApJ*, 440, 706
- Rest, A., Welch, D. L., Suntzeff, N. B., et al. 2008, *ApJL*, 681, L81
- Rest, A., Foley, R. J., Sinnott, B., et al. 2011, *ApJ*, 732, 3
- Ryan, E., Wagner, R. M., & Starrfield, S. G. 2001, *ApJ*, 548, 811
- Ryder, S. D., Murrowood, C. E., & Stathakis, R. A. 2006, *MNRAS*, 369, L32
- Ruiz-Lapuente, P., Comeron, F., Méndez, J., et al. 2004, *Nature*, 431, 1069
- Sana, H., de Mink, S. E., de Koter, A., et al. 2012, *Science*, 337, 444
- Sandberg, A., & Sollerman, J. 2009, *AAP*, 504, 525
- Schaefer, B. E., & Pagnotta, A. 2012, *Nature*, 481, 164
- Schweizer, F., & Middleditch, J. 1980, *ApJ*, 241, 1039
- Schlaflly, E. F., & Finkbeiner, D. P. 2011, *ApJ*, 737, 103
- Scott, D. M., Finger, M. H., & Wilson, C. A. 2003, *MNRAS*, 344, 412
- Searle, L. 1971, *ApJ*, 168, 41
- Shappee, B. J., Kochanek, C. S., & Stanek, K. Z. 2013, *ApJ*, 765, 150
- Smartt, S. J. 2009, *ARA&A*, 47, 63
- Smith, N., Li, W., Filippenko, A. V., & Chornock, R. 2011,

- MNRAS, 412, 1522
- Smith, N. 2013, MNRAS, 434, 102
- Tetzlaff, N., Neuhäuser, R., & Hohle, M. M. 2011, MNRAS, 410, 190
- Thorstensen, J. R., Fesen, R. A., & van den Bergh, S. 2001, AJ, 122, 297
- van den Bergh, S. 1980, Journal of Astrophysics and Astronomy, 1, 67
- van den Bergh, S., & Pritchett, C. J. 1986, ApJ, 307, 723
- Van Dyk, S. D., de Mink, S. E., & Zapartas, E. 2016, ApJ, 818, 75
- Woosley, S. E., Eastman, R. G., Weaver, T. A., & Pinto, P. A. 1994, ApJ, 429, 300
- Wu, C.-C. 1981, ApJ, 245, 581
- Yamaguchi, H., Badenes, C., Petre, R., et al. 2014, ApJL, 785, L27
- Yoon, S.-C., Woosley, S. E., & Langer, N. 2010, ApJ, 725, 940
- Yoon, S.-C., Gräfener, G., Vink, J. S., Kozyreva, A., & Izzard, R. G. 2012, AAP, 544, L11
- Yoon, S.-C., Dessart, L., & Clocchiatti, A. 2017, arXiv:1701.02089
- Young, P. A., Fryer, C. L., Hungerford, A., et al. 2006, ApJ, 640, 891
- Zacharias, N., Monet, D. G., Levine, S. E., et al. 2005, VizieR Online Data Catalog, 1297